

A thermodynamic description of colloidal glasses

MAURO SELLITTO¹ and FRANCESCO ZAMPONI²

¹ *Dipartimento di Ingegneria Industriale e dell'Informazione, Seconda Università di Napoli, Real Casa dell'Annunziata, I-81031 Aversa (CE), Italy*

² *Laboratoire de Physique Théorique, Ecole Normale Supérieure, UMR 8549 CNRS, 24 Rue Lhomond, 75005 Paris, France*

PACS 64.70.Q – Theory and modeling of the glass transition
PACS 61.43.Fs – Glasses
PACS 82.70.Dd – Colloids

Abstract. - The phase behavior of hard-sphere particles interacting with a short-ranged potential is studied in the limit of infinite space dimensionality via the Franz-Parisi approach and the replica method of disordered systems. For an attractive square-well potential the phase diagram exhibits reentrancy of the liquid-glass transition, multiple glass states and glass-glass transition. For a repulsive square shoulder potential no such special features are observed. Our results show that the Franz-Parisi approach can be consistently extended to deal with higher-order glass singularities and that interparticle attraction is crucial for complex glassy behavior in large enough dimensions, at least for monodisperse systems.

Introduction. – Interacting hard spheres (with weak long-range attraction) have been used since van der Waals to describe the gas-liquid phase transition. More recently, they have been much studied in relation with colloidal suspensions [1]. The interest has been especially motivated by the possibility of introducing a (depletion-induced) attraction between colloidal particles by adding a suitable amount of non-adsorbing polymers to the suspension [2]. In doing so the intensity and the range of attraction can be tuned by changing the polymer concentration and the polymer coil radius, respectively. One can thus explore a wide range of static and dynamic behaviors which are not accessible in a single liquid system. When the range of attraction is microscopic (i.e. of the order of a small fraction of the sphere diameter) some fascinating large-scale macroscopic properties emerge in such systems. They include the reversible freezing-by-heating of the liquid phase and, at higher packing density, structurally distinct types of dynamically arrested states [3–10]. Such features have been generally ascribed to structural changes of the cage that confines particle motion. For weak attraction and high packing density the glass formation is mainly driven by the usual excluded-volume effects, while for strong attraction the tight clustering of particles leads to an amorphous state with a rigid gel-like structure which can exist even at very low packing. The passage from one glass state to the other can occur either smoothly or discontinuously

(in the latter case the Debye-Waller factor undergoes an extra jump). Interestingly, similar complex glassy features have been also identified in systems with no attractive interaction [11–14], where distinct glass states with different packing properties arise solely from the competition between crowding effects on different microscopic length scales.

In this paper we investigate the statistical mechanics of interacting hard spheres in the case in which the space dimensionality is infinitely large. In statistical physics high-dimensional spaces are, in fact, a blessing. They make more feasible some computations [15,16] and, most importantly, provide a limiting case in which the various mean-field approximations become exact [16,17]. For this reason, the mean-field replica approach we use is exact [18,19] and this allows for a comparison with the results obtained by alternative methods, such as the Mode-Coupling Theory (MCT) [20,21], numerical simulations [3,5,6], experiments [7,8], spin glass (or lattice glass) models [22–26], and the heterogeneous facilitation picture [14,27,28]. We generally find that for short-range enough attraction the phase diagram exhibits reentrancy of the liquid-glass transition line, multiple glass states and glass-glass transition (much similar to those observed in colloid-polymer mixtures, numerical simulations and MCT), while for short-range repulsion no such special features is observed. Our results show that the static approach based on the Franz-

Parisi potential can be consistently generalized to higher-order dynamical glass singularities, and that attraction is an essential ingredient for observing complex glassy features in high dimensional spaces.

The model. – We consider a system of d -dimensional hard spherical particles of unit diameter interacting with an attractive potential of constant strength U_0 over a distance $\hat{\sigma}/d$:

$$v(r) = \begin{cases} \infty & \text{for } r < 1 \\ -U_0 & \text{for } 1 < r < 1 + \hat{\sigma}/d \\ 0 & \text{for } r > 1 + \hat{\sigma}/d \end{cases} \quad (1)$$

where r is the inter-particle distance. Note that, in order to have a non-trivial limit for $d \rightarrow \infty$, the width of the attractive part has been rescaled by the dimension according to the cage size dependence on d in the glass (i.e. proportionally to $1/d$), see [19] and Eq. (2) below.

For a system of density ρ in the thermodynamic limit, we define $\hat{\varphi} = 2^d \varphi/d$ where $\varphi = \frac{\pi^{d/2}}{\Gamma(1+d/2)} \rho$ is the packing fraction of the repulsive core. The motivation behind this scaling is that in the replica approach the glass transition occurs for values of $\hat{\varphi}$ that remain finite for $d \rightarrow \infty$ (e.g. in the pure hard sphere case the dynamical transition happens at $\hat{\varphi} = 4.8$ [19]). We observe that MCT gives a different scaling for the dynamical transition density, but numerical data seems to support the replica result [29]. Note, for comparison, that it can be proven that sphere packings exist at least for $\hat{\varphi} \leq 6/e$ [30], hence a $\hat{\varphi}$ of order 1 is a quite natural scale for hard spheres in large dimensions (see [19, 31] for a more detailed discussion).

Moreover, we fix $\beta U_0 = 1/\hat{T}$ where $\beta = 1/k_B T$. The control parameters are therefore rescaled density $\hat{\varphi}$, rescaled temperature \hat{T} and the width of the attraction $\hat{\sigma}$. In the following we will also consider a “sticky” or “Baxter” limit in which $\hat{\sigma} \rightarrow 0$ while the intensity of the attraction diverges, hence $\hat{T} \rightarrow 0$, while $\mu = -1/\hat{T} - \log \hat{\sigma}$ is held constant.

Franz-Parisi potential. – The basic idea of the replica approach to the glass transition is that the kinetic slowing down on approaching the glass phase is due to the sudden appearance of a bunch of long-lived metastable states [32–34]. Under this assumption, the glass transition can be identified by looking at the free energy of a *constrained* equilibrium system. This is known as the Franz-Parisi potential [35–37], see also [34, 38] for an alternative but very related approach. For particle systems, the best way of computing this potential explicitly is the following. One considers an equilibrium configuration $X = \{x_i^\alpha\}_{i=1, \dots, N}^{\alpha=1, \dots, d}$ of the liquid, and another configuration $Y = \{y_i^\alpha\}_{i=1, \dots, N}^{\alpha=1, \dots, d}$ that is constrained to be close to the first one, in such a way that the mean square displacement is bounded by a fixed constant \hat{A} :

$$\frac{1}{2d} \frac{1}{N} \sum_{\alpha=1}^d \sum_{i=1}^N \langle (x_i^\alpha - y_i^\alpha)^2 \rangle \leq \frac{\hat{A}}{d^2}. \quad (2)$$

One then computes the free energy of the system given X , and then averages it over the equilibrium distribution of X . The result is the average free energy $\mathcal{V}_{\text{FP}}(\hat{A})$ of a system constrained to be at distance \hat{A} from a typical liquid configuration. In the liquid phase, particles diffuse away from any reference configuration, and correspondingly $\mathcal{V}_{\text{FP}}(\hat{A})$ has a unique minimum at $\hat{A} = \infty$. On the contrary, in the glass phase, particles are “caged” in a sphere of average radius $\sqrt{\hat{A}}$ around the reference configuration and consequently there is a local minimum of $\mathcal{V}_{\text{FP}}(\hat{A})$ at finite \hat{A} . The *dynamical glass transition* $T_{\text{dyn}}(\varphi)$ is signaled by the appearance of an inflection point in $\mathcal{V}_{\text{FP}}(\hat{A})$, and hence the secondary minimum appears discontinuously at a finite \hat{A} below $T_{\text{dyn}}(\varphi)$, and therefore represents a generic *fold* singularity. From an analytic point of view, the computation of the Franz-Parisi potential requires the use of the replica method [19, 37, 39, 40]. Since our method is a direct extension of previous works [19, 41], we provide here only the final results of our computation.

The Franz-Parisi potential \mathcal{V}_{FP} can be obtained through the relation (more details of the derivation will be given in [42]):

$$\mathcal{V}'_{\text{FP}}(\hat{A}) = -\frac{1}{\hat{A}} \left[1 - \hat{\varphi} \mathcal{F}_1(\hat{A}) \right], \quad (3)$$

where

$$\mathcal{F}_1(\hat{A}) = -\hat{A} \int_{-\infty}^{\infty} dy e^y \frac{\partial q(\hat{A}; y)}{\partial \hat{A}} \log q(\hat{A}; y) \quad (4)$$

and the function $q(\hat{A}; y)$ is

$$q(\hat{A}; y) = (1 - e^{\hat{\sigma}_0}) \Theta \left(\frac{y + \hat{A} - \hat{\sigma}}{2\sqrt{\hat{A}}} \right) + e^{\hat{\sigma}_0} \Theta \left(\frac{y + \hat{A}}{2\sqrt{\hat{A}}} \right). \quad (5)$$

The stationary points of $\mathcal{V}_{\text{FP}}(\hat{A})$ are located at values of \hat{A} which are the solutions of $1/\hat{\varphi} = \mathcal{F}_1(\hat{A})$. The values of \hat{A} at the local minima represent the long-time mean square displacement (i.e. the Debye-Waller factor) in the glass. In this context the dynamical transition corresponds to the disappearance of all the local minima of $\mathcal{V}_{\text{FP}}(\hat{A})$, which happens when $\hat{\varphi}^{-1} > \max_{\hat{A}} \mathcal{F}_1(\hat{A})$. Hence, the dynamic transition is located at

$$\frac{1}{\hat{\varphi}_d} = \max_{\hat{A}} \mathcal{F}_1(\hat{A}), \quad (6)$$

and its stability requires the local (up) convexity of \mathcal{V}_{FP} . A phase diagram obtained in this *static* framework is therefore derived by studying the behavior of the functions \mathcal{V}_{FP} and \mathcal{F}_1 . Let us now consider two specific cases.

Square-well potential. – We first discuss the results obtained for the square-well attractive potential of width $\hat{\sigma}$ and depth U_0 . We find that when the attraction width is large enough (above $\hat{\sigma} \simeq 0.19$), the function \mathcal{F}_1 has a single maximum for all densities and temperatures, and the resulting phase structure is easily determined: for each

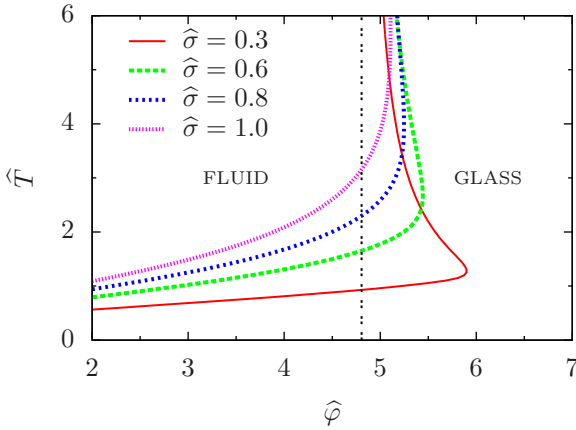


Fig. 1: A section of the phase diagram in the rescaled variables, temperature $\hat{T} = k_B T / U_0$ vs packing fraction $\hat{\varphi}$, for attraction width $\hat{\sigma}$. The vertical line is the packing fraction at the dynamic glass transition for the purely hard-sphere potential. In this case there is only one glass phase but the fluid-glass transition line is reentrant: the liquid freezes upon heating.

temperature, a single glass phase exists for densities larger than $\hat{\varphi}_d$ defined by Eq. (6).

In Fig. 1 we show the phase diagram in the rescaled variables: reduced temperature, $\hat{T} = k_B T / U_0$, and reduced packing fraction, $\hat{\varphi}$. Interestingly, for packing fractions above the dynamic glass transition of the purely hard-sphere system the liquid-glass transition line develops a reentrance: the liquid freezes upon heating. This reentrancy effect is driven by the width of the square-well potential and is ultimately due to entropic reasons. The smaller the attraction width the deeper the fluid phase enters into the glass region.

When the attraction width is below $\hat{\sigma} \simeq 0.19$, the function \mathcal{F}_1 shows two maxima in a range of temperatures and densities, and the determination of the phase diagram requires some care because of the appearance of multiple glass phases. For simplicity we focus on a representative case, obtained by fixing $\hat{\sigma} = 0.06$. The corresponding section of the phase diagram is shown in Fig. 2. There are two lines, A_3 -C and A'_3 -C separating the fluid phase from two distinct types of glass phase, named *attractive glass* (that with smaller \hat{A}) and *repulsive glass* (the one with larger \hat{A}). These lines, which correspond to the maxima of \mathcal{F}_1 , cross each other at the point C and terminate at the critical endpoints A_3 and A'_3 . The curve A_3 - A'_3 instead corresponds to the minima of \mathcal{F}_1 . The closed area delimited by the lines going through the points A_3 , C and A'_3 represents the coexistence region of the two glass phases, while outside this region only one glass is present. It is important to observe that the A'_3 point corresponds to a *local quartic maximum* of the Franz-Parisi potential: it is therefore dynamically unobservable as the repulsive glass will always be unstable around this singularity. On the contrary, the A_3 singularity corresponds to a *local quartic minimum* of

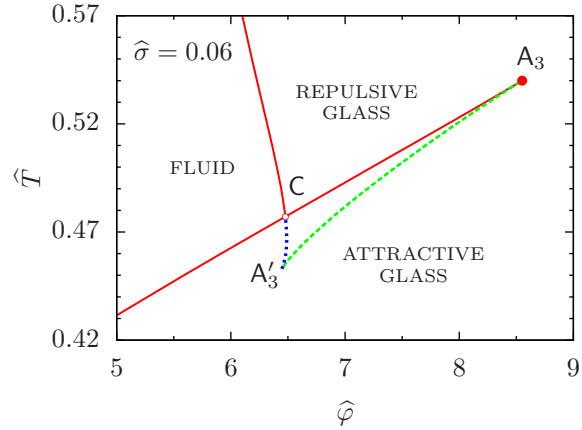


Fig. 2: Section of phase diagram at $\hat{\sigma} = 0.06$. There are two distinct types of glass phases and fluid-glass transitions plus a glass-glass transition line. The two fluid-glass transition lines meet at a crossing point C along with the glass-glass transition line. The two special points A_3 and A'_3 are cusp singularities whose stability is determined by the Franz-Parisi potential.

the Franz-Parisi potential, and is therefore stable. The detailed shape of \mathcal{V}_{FP} in the former case is shown in Fig. 3 for densities located at the intersection of the transition lines with the horizontal segment $\hat{T} = 0.47$. We notice that our conclusion is consistent with the results of MCT and, interestingly enough, that the MCT dynamic stability criterion is automatically built up in the Franz-Parisi potential: indeed, the minima of the Franz-Parisi potential correspond to dynamically stable solutions in MCT. This static approach can be therefore consistently extended to the determination of higher-order dynamic glass singularities.

For completeness we also show the related evolution of the cage radius $\sqrt{\hat{A}}$ as a function of the packing density in Fig. 4 at temperatures slightly above and below the C point. The double jump observed at $\hat{T} = 0.5$ represents the transition from the liquid to the repulsive glass followed, for increasing packing density, by the one from the repulsive glass to the attractive glass. As it happens with the usual first-order transition hysteresis effects between the two glass phases should be observed. At $\hat{T} = 0.47$ there is only the liquid-to-attractive glass transition. In this latter case if by any chance the appearance of the attractive glass is delayed, the liquid could momentarily transform into a repulsive glass.

Fig. 5 summarizes the global structure of the phase diagram in the two-glass region. Upon decreasing $\hat{\sigma}$ the glass-glass transition line shortens and eventually disappears at $\hat{\sigma} \approx 0.19$ where the A_3 cusp merges into a singularity of type A_4 , also known as swallowtail bifurcation. From Eq. (3) it is easy to see that at the stationary points of the potential, the vanishing of the ℓ -th derivative of $\mathcal{F}_1(\hat{A})$ leads to the vanishing of the $(\ell + 1)$ -th derivative of $\mathcal{V}_{FP}(\hat{A})$. The higher-order singularities, A_3 and A_4 , are

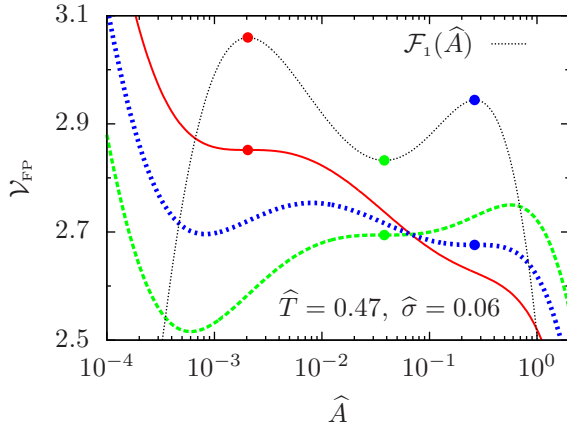


Fig. 3: Shape of the Franz-Parisi potential $\mathcal{V}_{\text{FP}}(\hat{A})$ and the function $\mathcal{F}_1(\hat{A})$ in the region below \hat{T}_C . The three $\mathcal{V}_{\text{FP}}(\hat{A})$ curves correspond to the points at which the phase diagram transition lines intersect the horizontal segment at $\hat{T} = 0.47$. The dots denote the stationary points of the function $\mathcal{F}_1(\hat{A})$ and the corresponding ones in $\mathcal{V}_{\text{FP}}(\hat{A})$. Notice that \mathcal{F}_1 does not depend on density while \mathcal{V}_{FP} does.

special singular points of the Franz-Parisi potential. Near these higher-order singularities peculiar slow logarithmic relaxation occurs, a behavior that has been explored in great detail in the MCT framework [3, 4] and numerically [3, 5, 6, 43, 44]. Fig. 5 also includes the Baxter (or sticky sphere) limit: $\hat{\sigma} \rightarrow 0$, $U_0 \rightarrow \infty$ (or equivalently $\hat{T} \rightarrow 0$) while $\mu = -\beta U_0 - \log \hat{\sigma} = -1/\hat{T} - \log \hat{\sigma}$ is kept constant. In this limit the small- \hat{A} maximum of $\mathcal{F}_1(\hat{A})$, corresponding to the attractive glass, moves to $\hat{A} = 0$, meaning that particles are completely frozen. The height of this maximum can be computed explicitly and gives $\hat{\varphi}_d = 2e^\mu$. Hence in this case the cusp singularity A_3 moves to infinite packing density. This implies that there is no smooth path in the phase diagram from the repulsive to the attractive glass. The resulting curve is reported in Fig. 5 as a full line. Notice that in the limit $d \rightarrow \infty$ the Kauzmann transition is pushed at infinite packing density and is therefore outside the range of physical relevance. Very similar phase diagrams have been first obtained by MCT [3, 4], and later confirmed by numerical simulations [5, 6] and experiments [7, 8]. In a previous attempt to use the replica method for this problem, based on the replicated Hypernetted Chain approximation and in $d = 3$, no glass-glass transition was found [45], arguably due to the rather poor accuracy of the replicated Hypernetted Chain approximation in the phase region where the “cage size” is very small [19].

Square-shoulder potential. – The analysis carried out above for the square-well potential can be immediately extended to the square-shoulder potential by exchanging $U_0 \rightarrow -U_0$. This case is interesting because it provides the first finite dimensional ($d = 3$) instance in which mul-

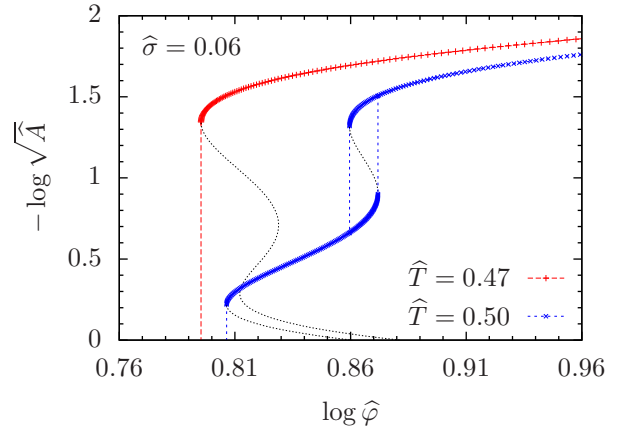


Fig. 4: Cage radius $\sqrt{\hat{A}}$ vs packing density $\hat{\varphi}$ for attraction width $\hat{\sigma} = 0.06$ and temperatures slightly below and above the point C.

tipple glasses are observed with only purely repulsive potential [11]. Similar features have been recently obtained also in some binary mixtures [12] and in the heterogeneous facilitation approach [14]. The phase diagram for the square-shoulder potential in infinite dimension is reported in Fig. 6. Perhaps surprisingly, we find no trace of distinct glasses but only the obvious widening of the glass phase when the repulsion gets stronger (or the temperature is lowered) and the interaction range increases.

This negative result suggests that the contribution of “ring diagrams”, which vanish in the limit of high dimensionality [19, 46], is relevant for the appearance of multiple glasses in purely repulsive potential in finite dimension d . Indeed, in Ref. [11] it is argued that the complex phase diagram of the square-shoulder potential is intimately connected to the competition between the amplitudes of the jumps of the pair correlation $g(r)$ at the two contact points corresponding to the two singularities of the potential (see Fig. 3 and the associated discussion in Ref. [11]). This effect, that is clearly observed in $d = 3$, disappears in infinite dimensions where all ring diagrams vanish: in this case, in the liquid phase, one has $g(r) = \exp[-\beta v(r)]$, the structure of $g(r)$ is much simpler, and in particular the value of $g(r)$ at the first contact decreases on increasing the attraction strength and is always lower than the one at the second contact. Clearly, the richer structure of $g(r)$ in $d = 3$, which is responsible for the complex phase diagram of the square-shoulder potential, is due to the contribution of ring diagrams (i.e., many-body effects) which are absent in infinite dimensions.

This leads us to conclude that, while the complex phase diagram of the square-well attractive potential is well accounted for by the simple two-body mean field approximation in infinite dimensions, capturing the same physics for the square-shoulder potential requires the inclusion of (static) many-body effects that are only present in low enough dimensions [11]. These are automatically imple-

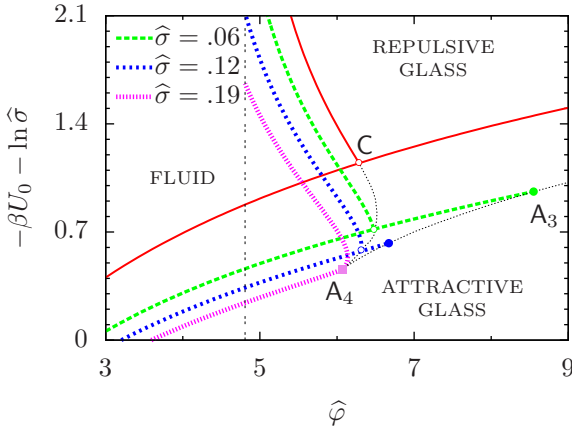


Fig. 5: Global phase diagram in the two-glass region for several values of $\hat{\sigma}$. The sticky limit is represented by a full line. The two dotted light lines departing from the swallowtail bifurcation A_4 are the line of cusp singularities A_3 (represented as full dots) the line of crossing points C (empty dots).

mented in MCT through the static structure factor of the liquid which is taken as input of the theory; the same can be done in principle in the replica approach but it requires a systematic improvement of the simplest approach used in this paper, along the lines discussed in [19].

Conclusion. — The main result of this paper is that a static replica picture based on the Franz-Parisi potential allows to re-derive many of the results that have been previously obtained using MCT for attractive colloids [3, 4, 9], namely the reentrance of the glass transition line and two distinct glass phases for very short range attractions. Here we limited ourselves to the $d \rightarrow \infty$ limit where computations are easier and the replica theory is exact [18], at least according to the standards of theoretical physics. For soft matter applications, one would like of course to extend this calculation in $d = 3$ [19]. We expect that the phase diagram will remain qualitatively the same, at least for the square-well attractive potential. For the square-shoulder potential, we expect that including properly the finite dimensional contributions should allow one to recover the complex phenomenology discovered in [11]. Unfortunately, constructing a good approximation scheme for the dynamical transition in low dimensions within the small cage expansion scheme is a non-trivial task, but there is hope to achieve it and work is in progress in this direction. Moreover, one could compute within this framework the equation of state of the two glasses, the jump of specific heat at the glass transition, and address the role of the Kauzmann transition.

This work originated in Ein Gedi during the Italo-Israelian bilateral meeting on *Statistical Physics of Glass Formation and Amorphous Solids*. We thank R. Benzi,

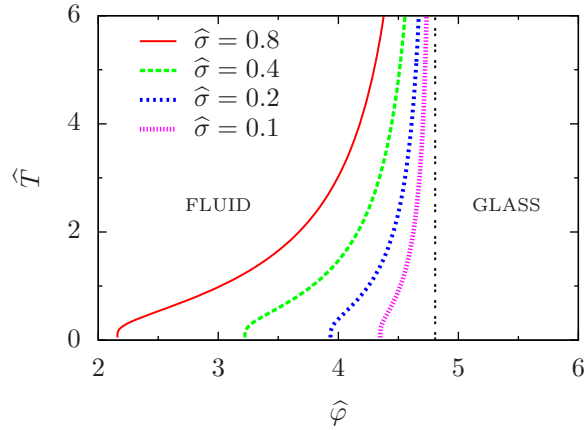


Fig. 6: Phase diagram for the square-shoulder repulsive potential for several values of the width $\hat{\sigma}$.

G. Parisi and I. Procaccia for that opportunity. We also thank P. Charbonneau and E. Zaccarelli for many useful discussions.

REFERENCES

- [1] PUSEY P. N., *Colloidal Suspensions in Liquids, Freezing and Glass Transition*, edited by HANSEN J. P., LEVEQUE D. and ZINN-JUSTIN J., (North-Holland) 1991.
- [2] POON W. C., *J. Phys.: Condens. Matter*, **14** (2002) R859.
- [3] DAWSON K., FOFFI G., FUCHS M., GÖTZE W., SCIORTINO F., SPERL M., TARTAGLIA P., VOIGTMANN T. and ZACCARELLI E., *Phys. Rev. E*, **63** (2000) 011401.
- [4] GÖTZE W., *Complex dynamics of glass-forming liquids: A mode-coupling theory* (Oxford University Press, USA) 2009.
- [5] ZACCARELLI E. and POON W. C., *Proceedings of the National Academy of Sciences*, **106** (2009) 15203.
- [6] FOFFI G., SCIORTINO F., ZACCARELLI E. and TARTAGLIA P., *Journal of Physics: Condensed Matter*, **16** (2004) S3791.
- [7] ECKERT T. and BARTSCH E., *Phys. Rev. Lett.*, **89** (2002) 125701.
- [8] PHAM K. N., PUERTAS A. M., BERGENHOLTZ J., EGELHAFF S. U., MOUSSAID A., PUSEY P. N., SCHOFIELD A. B., CATES M. E., FUCHS M. and POON W. C., *Science*, **296** (2002) 104.
- [9] SCIORTINO F., *Nature materials*, **1** (2002) 145.
- [10] FRENKEL D., *Science*, **296** (2002) 65.
- [11] SPERL M., ZACCARELLI E., SCIORTINO F., KUMAR P. and STANLEY H. E., *Phys. Rev. Lett.*, **104** (2010) 145701.
- [12] VOIGTMANN T., *Europhys. Lett.*, **96** (2011) 36006.
- [13] DAS G., GNAN N., SCIORTINO F. and ZACCARELLI E., *J. Chem. Phys.*, **138** (2013) 134501.
- [14] SELLITTO M., *J. Chem. Phys.*, **138** (2013) 224507.
- [15] CALLEN H. B., *Thermodynamics and an Introduction to Thermostatistics* (J. Wiley & Sons, New York) 1985.
- [16] PELITI L., *Statistical Mechanics in a Nutshell* (Princeton University Press, Princeton) 2011.
- [17] PARISI G., *Statistical Field Theory* (Addison-Wesley, Reading) 1988.

- [18] KURCHAN J., PARISI G. and ZAMPONI F., *Journal of Statistical Mechanics: Theory and Experiment*, **2012** (2012) P10012.
- [19] PARISI G. and ZAMPONI F., *Rev. Mod. Phys.*, **82** (2010) 789.
- [20] BERGENHOLTZ J. and FUCHS M., *Phys. Rev. E*, **59** (1999) 5706.
- [21] FABBIAN L., GÖTZE W., SCIORTINO F., TARTAGLIA P. and THIERY F., *Phys. Rev. E*, **59** (1999) R1347.
- [22] CAIAZZO A., CONIGLIO A. and NICODEMI M., *Phys. Rev. Lett.*, **93** (2004) 215701.
- [23] CRISANTI A. and LEUZZI L., *Phys. Rev. B*, **73** (2006) 014412.
- [24] KRAKOWIACK V., *Phys. Rev. B*, **76** (2007) 136401.
- [25] CRISANTI A. and LEUZZI L., *Phys. Rev. B*, **76** (2007) 136402.
- [26] KRZAKALA F., TARZIA M. and ZDEBOROVÁ L., *Physical Review Letters*, **101** (2008) 165702.
- [27] SELLITTO M., DE MARTINO D., CACCIOLI F. and ARENZON J. J., *Phys. Rev. Lett.*, **105** (2010) 265704.
- [28] SELLITTO M., *Phys. Rev. E*, **86** (2012) 030502.
- [29] CHARBONNEAU PATRICK, and IKEDA ATSUSHI, and PARISI GIORGIO, and ZAMPONI FRANCESCO, *Phys. Rev. Lett.*, **107** (2011) 185702.
- [30] VANCE STEPHANIE, *Advances in Mathematics*, **227** (2011) 2144.
- [31] TORQUATO S. and STILLINGER F. H., *Rev. Mod. Phys.*, **82** (2010) 2633.
- [32] KIRKPATRICK T. R. and WOLYNES P. G., *Phys. Rev. A*, **35** (1987) 3072.
- [33] KIRKPATRICK T. R. and THIRUMALAI D., *Phys. Rev. A*, **37** (1988) 4439.
- [34] KIRKPATRICK T. R. and THIRUMALAI D., *Journal of Physics A: Mathematical and General*, **22** (1989) L149.
- [35] FRANZ S. and PARISI G., *Journal de Physique I*, **5** (1995) 1401.
- [36] FRANZ S. and PARISI G., *Phys. Rev. Lett.*, **79** (1997) 2486.
- [37] CARDENAS M., FRANZ S. and PARISI G., *Journal of Physics A: Mathematical and General*, **31** (1998) L163.
- [38] MONASSON R., *Phys. Rev. Lett.*, **75** (1995) 2847.
- [39] MÉZARD M. and PARISI G., *Journal of Physics A: Mathematical and General*, **29** (1996) 6515.
- [40] MÉZARD M. and PARISI G., *Glasses and replicas in Structural Glasses and Supercooled Liquids: Theory, Experiment and Applications*, edited by P.G.WOLYNES and V.LUBCHENKO, (Wiley & Sons) 2012.
- [41] BERTHIER L., JACQUIN H. and ZAMPONI F., *Phys. Rev. E*, **84** (2011) 051103.
- [42] SELLITTO M. and ZAMPONI F., *in preparation*, (2013) .
- [43] CHARBONNEAU P. and REICHMAN D. R., *Phys. Rev. Lett.*, **99** (2007) 135701.
- [44] SCIORTINO F., TARTAGLIA P. and ZACCARELLI E., *Phys. Rev. Lett.*, **91** (2003) 268301.
- [45] VELENICH A., PAROLA A. and REATTO L., *Physical Review E*, **74** (2006) 021410.
- [46] FRISCH H. L. and PERCUS J. K., *Phys. Rev. E*, **60** (1999) 2942.